Published 2001 Wiley-Liss, Inc.†

Rapid Communication

Fluorescence Resonance Energy Transfer Analysis of Cell Surface Receptor Interactions and Signaling Using Spectral Variants of the Green Fluorescent Protein

Francis Ka-Ming Chan[1], Richard M. Siegel[1], David Zacharias[3], Ruth Swofford[2], Kevin L. Holmes[2], Roger Y. Tsien[3], and Michael J. Lenardo[1]*

[1]Laboratory of Immunology, National Institute of Allergy and Infectious Diseases, National Institutes of Health, Bethesda, Maryland

[2]Flow Cytometry Section, National Institute of Allergy and Infectious Diseases, National Institutes of Health, Bethesda, Maryland

[3]Howard Hughes Medical Institute and Department of Pharmacology, University of California, San Diego School of Medicine, La Jolla, California

Received 17 November 2000; Accepted 5 May 2001

Background: Fluorescence resonance energy transfer (FRET) is a powerful technique for measuring molecular interactions at Ångstrom distances. We present a new method for FRET that utilizes the unique spectral properties of variants of the green fluorescent protein (GFP) for large-scale analysis by flow cytometry.

Methods: The proteins of interest are fused in frame separately to the cyan fluorescent protein (CFP) or the yellow fluorescent protein (YFP). FRET between these differentially tagged fusion proteins is analyzed using a dual-laser FACSVantage cytometer.

Results: We show that homotypic interactions between individual receptor chains of tumor necrosis factor receptor (TNFR) family members can be detected as FRET from CFP-tagged receptor chains to YFP-tagged receptor chains. Noncovalent molecular complexation can be detected as FRET between fusions of CFP and YFP to either the intracellular or extracellular regions of the receptor chains. The specificity of the assay is demonstrated by the absence of FRET between heterologous receptor pairs that do not biochemically associate with each other. Interaction between a TNFR-like receptor (Fas/CD95/Apo-1) and a downstream cytoplasmic signaling component (FADD) can also be demonstrated by flow cytometric FRET analysis.

Conclusions: The utility of spectral variants of GFP in flow cytometric FRET analysis of membrane receptors is demonstrated. This method of analyzing FRET allows probing of noncovalent molecular interactions that involve both the intracellular and extracellular regions of membrane proteins as well as proteins within the cells. Unlike biochemical methods, FRET allows the quantitative determination of noncovalent molecular associations at Ångstrom level in living cells. Moreover, flow cytometry allows quantitative analyses to be carried out on a cell-by-cell basis on large number of cells. Cytometry 44: 361–368, 2001. Published 2001 Wiley-Liss, Inc.†

Key terms: FRET; flow cytometry; GFP; TNF receptor; PLAD

Fluorescence resonance energy transfer (FRET) is a principle by which a fluorophore (donor) in an excited state transfers energy to a neighboring fluorophore (acceptor) through dipole-dipole interaction. FRET can be an accurate measurement of molecular proximity at Ångstrom distances (1,2). Application of FRET to the study of biologically important molecular interactions flourished in the 1980s with the advent of monoclonal antibody technology. Unlike conventional biochemical methods, the use of differentially labeled monoclonal antibodies in FRET analysis allows the elucidation of cell surface receptor interactions in living cells (3–6). It has been useful in

Grant sponsor: Miriam and Benedict Wolf/Cancer Research Institute.

*Correspondence to: Michael J. Lenardo, Laboratory of Immunology, National Institute of Allergy and Infectious Diseases, National Institutes of Health, Building 10, Room 11N311, Bethesda, MD 20892-1892.

E-mail: mlenardo@nih.gov

identifying relevant molecular interactions in a number of systems including the association between the T-cell receptor and CD4 upon antigen stimulation (7,8), between EGF receptor chains (9), and among the IL-2 receptor subunits (10). FRET has also been used to visualize ligand-receptor interactions between IL-1 and IL-1 receptors (11). However, the utility of this technique is limited by the availability of monoclonal antibodies that recognize epitopes of the receptor where maximum energy transfer can occur without disrupting the interactions under examination. Moreover, the analysis is limited to probing proximity of the extracellular region of cell surface receptors and cannot be used to quantify molecular associations occurring inside living cells.

The green fluorescent protein (GFP) isolated from jellyfish *Aequorea victoria* is a useful marker in cell biology and biochemistry (12). Distinct spectral variants of GFP have been described that show altered excitation and emission frequencies and may be suitable as complementary fluorescence donors and acceptors in FRET analysis. For example, the emission spectrum of blue fluorescent protein (BFP) overlaps with the excitation spectrum of GFP and may be an ideal pair for FRET analysis. In fact, chimeric proteins with BFP and GFP has been used to determine molecular interactions between dimeric subunits of the transcription factor Pit-1 (13) and between the survival protein Bcl-2 and its pro-apoptotic counterpart Bax (14). This blue and green FRET pair has also been used as a powerful indicator of intracytoplasmic calcium signaling (15). However, the usefulness of BFP is limited by its weak fluorescence. Nevertheless, these studies demonstrate the potential of spectral variants of GFP in FRET analysis without the use of monoclonal antibody probes.

Recently, two spectral variants of GFP, the cyan fluorescent protein (CFP) and the yellow fluorescent protein (YFP), have been described that show promising spectral properties for FRET (12). We tested CFP and YFP proteins for their applicability in flow cytometric FRET analysis by fusing them to the various members of the tumor necrosis factor receptor (TNFR) superfamily. The TNFRs are crucial regulators of immune homeostasis and have been shown to biochemically associate in a receptor-specific manner through a domain at the NH_2-terminal of the receptor called the PLAD (pre-ligand-binding assembly domain) (16–19). In this report, specific interactions of the TNFRs are detected between homotypic receptor pairs as well as between receptor and downstream signaling proteins using flow cytometric FRET analysis. Our results demonstrate that flow cytometric FRET analysis using the CFP and YFP pair is feasible and can be a powerful, easy, and efficient technique for studying molecular interactions in living cells.

MATERIALS AND METHODS

Flow Cytometer Setup

Cells were analyzed on a Becton Dickinson (San Jose, CA) FACS Vantage SE flow cytometer equipped with an ILT air-cooled argon laser and a Spectra Physics model 2060 krypton laser, equipped with violet optics. The argon laser was tuned to 514 nm for direct excitation of YFP and the krypton laser was tuned to 413 nm for excitation of CFP. We also found that the more standard 488 nm wavelength is adequate for YFP excitation but does not excite CFP (data not shown). Forward and side scatter filters were replaced with 513/10 bandpass filters. CFP was detected using a 470/20 nm bandpass filter in P6 (FL5). YFP emission resulting from direct excitation at 514 nm was detected in the P3 PMT using a 546/10 nm bandpass filter and emission caused by FRET was detected in P5 (FL4). A 505LP dichroic mirror (DM) was used for separating CFP and YFP (FRET) emission between P5 and P6. Electronic compensation was performed to remove CFP emission in the YFP-FRET detector (P5–P6). In addition, interlaser compensation was performed using the Omnicomp circuitry to remove YFP emission caused by excitation of YFP by the 413-nm krypton laser line. In order to perform this compensation, it was necessary to direct the current output of the P3 PMT into the P7 circuit so that P5–P7 interlaser compensation could be performed (Fig. 1). All of the data were collected with the fluidics pressurized to 29–30 pounds per square inch (psi). This was done to shorten the pulse timing between the argon at position 1 and the krypton at position 3 in order to perform interlaser compensation using the standard delay module equipped with a maximum delay of 17.5 μs. It was subsequently determined that comparable data could be obtained with the fluidics pressurized to 12 psi and substituting a delay module equipped with a maximum delay of 22.5 μs (data not shown). A total of 25,000 live cells were collected and analyzed for each sample.

Fluorescence Dequenching and FRET Calculations

293T cells were transfected on coverslips and examined using an inverted epifluorescence microscope with a 525/40 nm bandpass filter. To photobleach YFP, the samples were irradiated for 2–3 min. Under these conditions, direct bleaching of the CFP donor is kept to a minimum. The increase or dequenching of CFP emission is a direct measure of the FRET efficiency (E%):

$$E\% = [1 - (\textit{CFP emission before YFP photobleach}/\textit{CFP emission after YFP photobleach})] \times 100$$

Plasmid Construction

The construction of intracellular CFP and YFP fusions to p60 and p80 were described previously (16). For the extracellular fusions, CFP or YFP coding sequences were cloned into p60 or p80 by standard PCR to generate CFP_2- or YFP_2-p60 or p80 and CFP_{15}- or YFP_{15}-p60 or CFP_{10}(or YFP_{10})-p80. For the FADD-YFP construct, the COOH-terminal region of FADD containing the death domain (amino acids 80–220) was cloned in frame into the SalI/BamHI sites of the vector pEYFP-C1 (Clontech, CA), placing YFP at the NH_2-terminal end of the protein, in place of the death-effector domain.

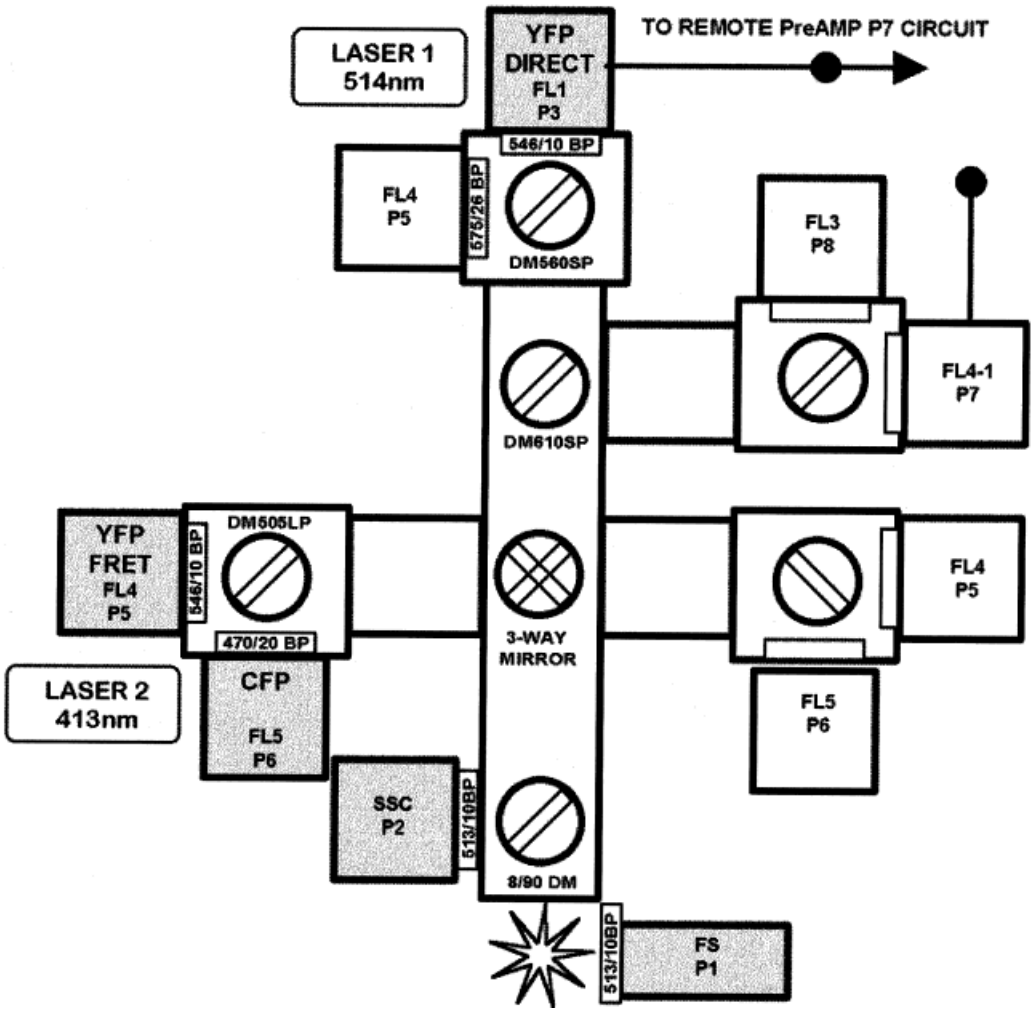

FIG. 1. Schematic for the FACS Vantage SE flow cytometer setup. Schematic diagram of optical pathway used for YFP and CFP detections (pertinent detectors shown in gray). Emission of YFP by direct 514 nm excitation is detected in FL1 (P3) and output is redirected to the circuit normally reserved for P7. Emission of CFP by 413 nm excitation is detected in FL5 (P6) and YFP emission due to FRET is detected in FL4 (P5). Spatial separation of laser beams is maintained in optical pathway by three-way mirror assembly. Bandpass filters and dichroic mirrors (DM) specifications are indicated. Note the 513/10 bandpass filters for forward scatter (FS) and side scatter (SSC), which are required with the argon laser tuned to 514 nm.

Transfections

All transfections were performed in the human embryonic kidney cell line 293T with Fugene 6 (Boehringer Mannheim, Indianapolis, IN). Cells were harvested 24–48 h posttransfection by resuspension in PBS supplemented with 2% FCS. Recombinant human TNFα (R&D Systems, Minneapolis, MN) was used at 100 ng/ml.

Data Analysis

All data analysis was performed using the program FlowJo (TreeStar Inc., San Carlos, CA). Because the FRET acceptor YFP is expressed in excess of the donor CFP, the CFP positive population (which is also positive for YFP) is gated for the determination of FRET in histogram analyses. Because of CFP quenching during FRET, normalizing FRET signal to CFP fluorescence may also be performed to determine the extent of FRET independent of receptor density.

RESULTS

We have previously identified an NH_2-terminal domain in the extracellular domain (ECD) of receptors in the TNFR superfamily termed PLAD (pre-ligand-binding assembly domain) that mediates ligand-independent homo-oligomeric receptor association (16,17). To determine the interaction of TNFR chains in living cells via the PLAD, we generated TNFR chimeras to either the CFP or YFP proteins (Fig. 2). Cells expressing p60 (TNFR-1)-CFP and p60-YFP (Fig. 3A, panel a) exhibited energy transfer as demonstrated by an increase in the FRET parameter (P5/FL4) compared to the control CFP only cells (Fig. 3B, panel a). This energy transfer could be enhanced in the presence of its cognate ligand TNFα (Fig. 3B, panel a, bold line). Replacing the fluorescence donor or acceptor with the heterologous DR4-CFP or DR4-YFP resulted in no FRET (Fig. 3B, panels b and d), although coexpression of

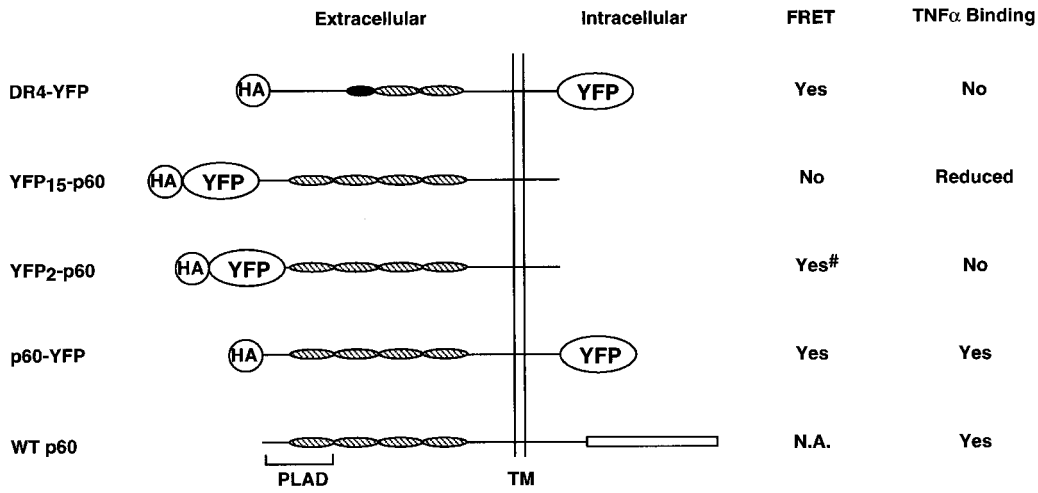

FIG. 2. Schematic of the different receptor fusions. Constructs used in the experiments. The hatched ovals represent the cysteine-rich domains (CRDs) of the TNFRs. The solid oval in DR4 represents the incomplete CRD that is also present in some other TNFR family receptors including Fas. The rectangular box represents the cytoplasmic death domain of p60. The pre-ligand-binding assembly domain (PLAD) of p60 and the HA epitope tag are shown. YFP_2-p60 and YFP_{15}-YFP are NH_2-terminal fusions with 2a.a. linker or 15a.a. linker, respectively. Only the YFP constructs are shown; the CFP constructs are exactly analogous. The two columns on the right summarize the FRET and ligand binding properties of the receptor fusions. For FRET analysis, FRET is defined as energy transfer between the indicated YFP fusion and its corresponding CFP counterpart. # FRET between CFP_2-p60 and YFP_2-p60 is only observed in the YFP-high population (see text). TM, transmembrane region. The domains are not drawn to scale.

DR4-CFP and DR4-YFP were capable of FRET (Fig. 3B, panel c). Therefore, FRET is only observed with homotypic interactions, which is consistent with biochemical analyses (16). The results from the flow cytometric analysis correlate with the results obtained from microscopic analysis of CFP dequenching (Fig. 3C). In this analysis, the difference of donor CFP fluorescence before and after photobleaching of the acceptor YFP gives a quantitative measurement of energy transfer (E%) between CFP and YFP fusion receptors. Cells coexpressing p60-CFP and p60-YFP or DR4-CFP and DR4-YFP gave E% of 7.46 and 9.78, respectively (Fig. 3C). Cells expressing heterologous receptor pairs failed to yield a significant E%. Taken together, these results demonstrate that CFP and YFP can be adapted to monitor specific, albeit noncovalent and low affinity associations, using the flow cytometer.

We next sought to determine if flow cytometric analysis of FRET between CFP and YFP was feasible when they are expressed on the outside of the cell. To this end, we constructed chimeric receptors that have the CFP or YFP fused to the NH_2-terminus of the ECDs of TNFRs. Two types of each of the NH_2-terminal fusions were tested; versions that had only two amino acid residues separating the CFP/YFP from the PLAD of the receptor (CFP_2 or YFP_2) and others with longer linkers (CFP_{15}-p60/YFP_{15}-p60 and CFP_{10}-p80 (TNFR-2)/YFP_{10}-p80) (Fig. 2). Interestingly, coexpression of CFP_2-p60 and YFP_2-p60 resulted in two distinct populations of cells that could be identified on the basis of their YFP fluorescence (Fig. 4A, panel a). Although the majority of the cells expressed lower level of YFP, a subpopulation of the CFP positive cells exhibited YFP fluorescence comparable to that observed with the intracellular fusion p60-YFP (Fig. 4A, cf. gates 1 and 2 in panels a and d). When these two populations of cells with differential YFP fluorescence were compared for energy transfer, FRET was observed only in the YFP high population (Fig. 4B, panel a). This confirms a requirement for at least a slight excess of acceptor to facilitate efficient FRET. The FRET observed between the ECD receptor fusions is specific because no FRET occurred between the heterologous TNFR-like receptor fusions CFP-Fas and YFP_2-p60 (Fig. 4B, panel b). The signal is also distance dependent as there was no FRET when the intracellular fusion p60-CFP and the ECD fusion YFP_2-p60 were coexpressed (Fig. 4B, panel c).

We found that the fluorescence of the YFP_2-p60 protein was greatly diminished, suggesting that the linker length between YFP and the fusion partner might have been too short for the proper folding of the protein (Fig. 5A). Comparison of the NH_2-terminal fusion YFP_2-p60 and the intracellular fusion p60-YFP showed a 10-fold decrease of YFP fluorescence for YFP_2-p60. Increasing the linker length by 13 amino acid residues (YFP_{15}-p60) did not dramatically enhance the YFP fluorescence (Fig. 5A). Similar analyses of the p80 TNFR fusions showed an even more dramatic decrease in fluorescence intensity when the YFP moiety was placed in the ECD (Fig. 5B). In this case, YFP_2-p80 exhibited a 100-fold decrease in fluorescence intensity compared to p80-YFP. A significant improvement in YFP fluorescence was observed when an additional eight amino acid residues were inserted in the linker for NH_2-terminal p80 fusion (YFP_{10}-p80; Fig. 5B). Similar results were obtained for the CFP fusions (data not shown). Thus, the proximity of CFP and YFP to the NH_2-terminal PLAD domain affects the fluorescence intensity of CFP and YFP fusion proteins.

The diminished fluorescence of YFP caused by the proximity of YFP to the TNFRs led us to consider

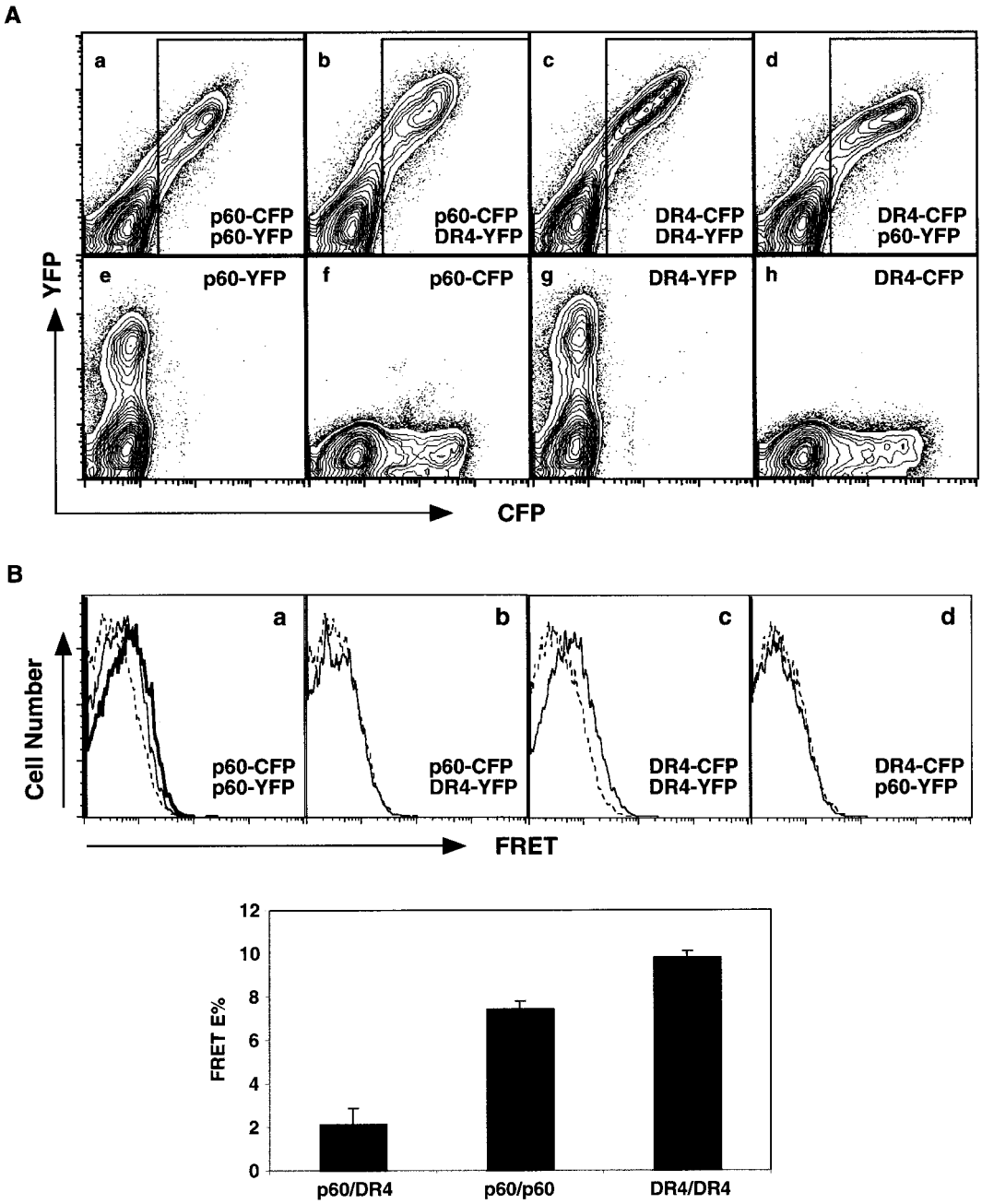

FIG. 3. Flow cytometric analysis of intracellular domain fusions. 293T cells were transfected with the indicated receptor fusion plasmids. **(A)** Contour plots analysis (with dots showing the outlier cell populations) of the fluorescence emission of CFP in relation to that of YFP. The rectangles in panels a–d denote the CFP positive gates whose cells were analyzed for FRET intensity in (B). **(B)** Histogram analysis of FRET between different CFP and YFP pairs. The dashed lines represent background FRET in the absence of YFP. The normal lines represent FRET in the presence of both CFP and YFP fusion proteins. The bold line in (a) represents the increased FRET between p60-CFP and p60-YFP in the presence of TNFα. 25,000 live cells were analyzed. **(C)** Microscopic dequenching analysis of CFP fusions. The E% represents the percent efficiency of FRET calculated as described in Materials and Methods. FRET between p60-CFP/p60-YFP, and DR4-CFP/DR4-YFP, was determined to be density-independent (data not shown). In all cases, at least three independent experiments were performed.

whether fusion of CFP or YFP adjacent to the PLAD may alter the function of the TNFRs. To this end, we assessed the effects of ECD receptor fusions on ligand binding by the receptor. Intracellular fusions of CFP or YFP to p60 or p80 did not alter ligand binding by the receptor (data not shown). However, fusion of YFP at the NH_2-termini of p60 or p80 severely hampered the ligand binding capacity of the receptor (Fig. 5C, cf. panels a–c and d–f). This effect on TNFα binding is also sensitive to the linker length between YFP and the

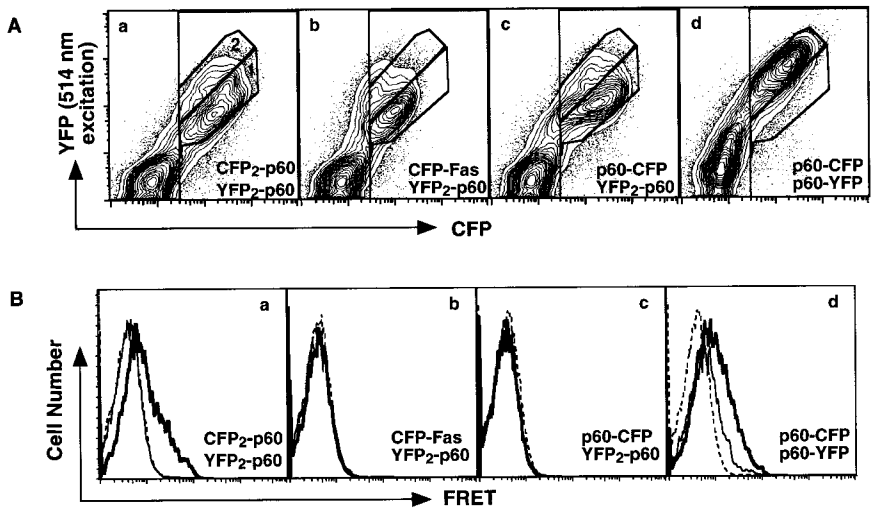

FIG. 4. Flow cytometric analysis of extracellular domain fusions. 293T cells were transfected with the indicated receptor fusions. **(A)** Two-dimensional contour plot analysis of CFP and YFP fluorescence intensities. The two different gates used for histogram analysis in (B) are shown. Gates 1 and 2 represent the YFP-low and YFP-high populations respectively. **(B)** Histogram analysis of FRET for the different CFP and YFP pairs shown in (A). The dashed lines represent FRET in the absence of YFP for the CFP positive cells. The normal lines represent FRET of the CFP-positive, YFP-low cells (gate 1). The bold lines represent FRET of the CFP-positive, YFP-high cells (gate 2). 25,000 live cells were analyzed for each sample.

PLAD. While both YFP_2-p60 (Fig. 5C, panel c) and YFP_2-p80 (Fig. 5C, panel f) showed barely detectable TNFα binding, YFP_{15}-p60 exhibited reduced, yet significant ligand binding (Fig. 5C, panel b). Despite a longer linker, YFP_{10}-p80 still failed to show appreciable binding to TNFα, suggesting that this receptor may be more sensitive to the effect of the fusion (Fig. 5C, panel e). Studies with the CFP fusions yielded similar results (data not shown). Thus, ECD fusions of CFP or YFP with receptor chains can significantly perturb receptor-li-

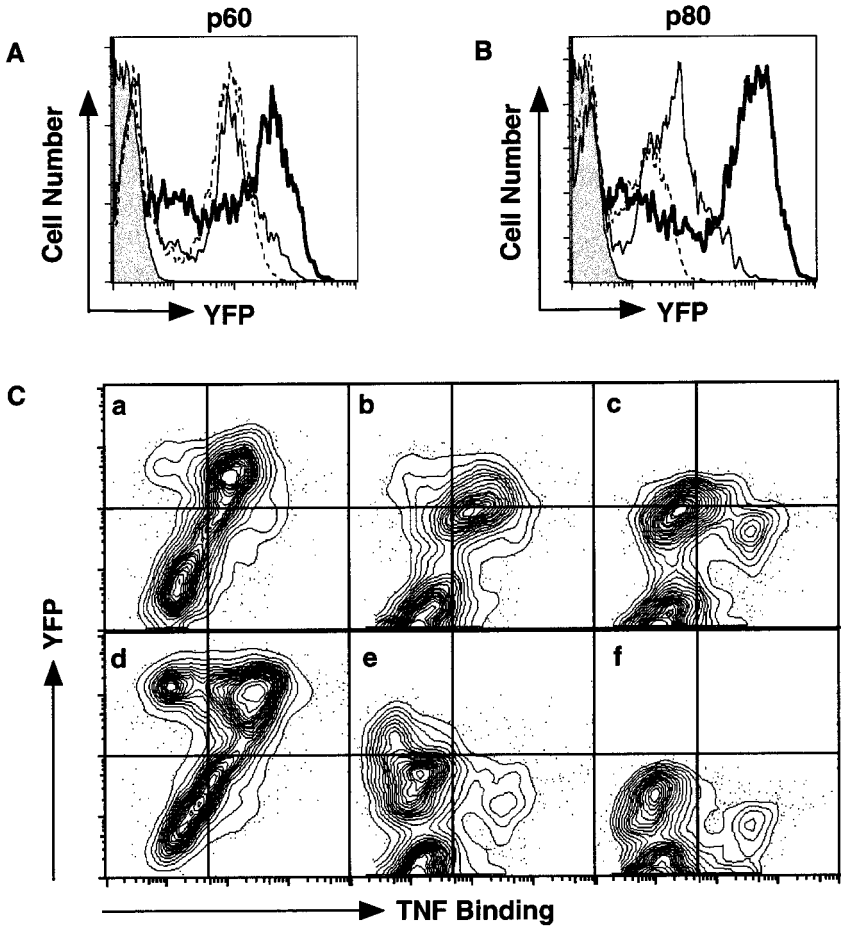

FIG. 5. The distance between YFP and TNFR affects YFP fluorescence and TNFR ligand binding. The fluorescence intensities of **(A)** p60 and **(B)** p80 ECD fusions with YFP. The shaded areas represent the background fluorescence of mock transfected 293T cells. The dashed lines denote the ECD fusions with the short spacer (YFP_2-p60 and YFP_2-p80). The normal lines represent the ECD fusions with the long spacer (YFP_{15}-p60 and YFP_{10}-p80). The bold lines represent the intracellular fusions (p60-YFP and p80-YFP). **(C)** Contour plot analysis of YFP fluorescence and TNFα binding by the various TNFR-YFP fusion receptors. 293T cells were transfected with (a) p60-YFP, (b) YFP_{15}-p60, (c) YFP_2-p60, (d) p80-YFP, (e) YFP_{10}-p80, and (f) YFP_2-p80. TNFα binding was determined using biotinylated TNFα (NEN Life Science Products, Inc.) and PE-conjugated streptavidin. FACS analysis was performed using the standard FAC Scan with a standard 488 nm laser.

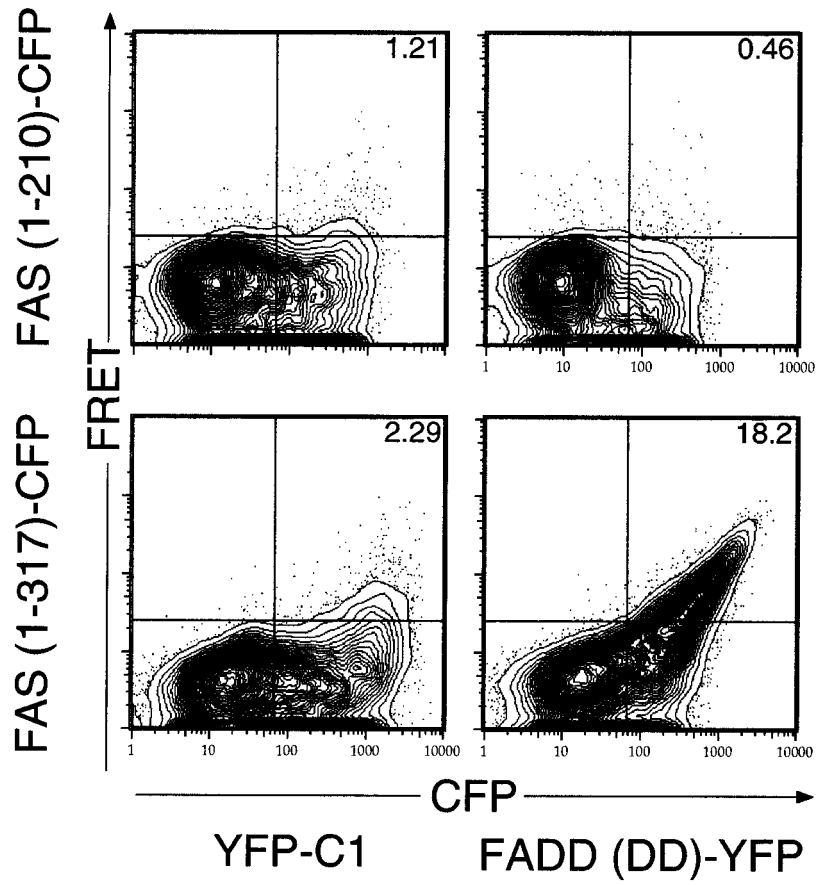

FIG. 6. Interaction between Fas and FADD death domains visualized by FRET. Plasmids encoding the full-length (1–317) or death-domain deleted Fas (1–210) fused to CFP at the COOH-terminus (17) were cotransfected with the YFP expression vector YFP-C1 (Clontech) or a vector encoding a FADD (DD)-CFP fusion protein as indicated. YFP was coexpressed with CFP in >80% of the cells in all panels. The number in the upper right quadrant of each plot represents the percentage of CFP positive cells that exhibit FRET.

gand interactions, which will be important to consider when using this technique.

To determine whether FRET analysis can be used to detect recruitment of intracellular signaling proteins to TNFR-family receptors, we analyzed the interaction between Fas and FADD death domains (DDs). The FADD adapter protein is known to be recruited to the DD of Fas after ligand binding through a homologous DD in the COOH-terminal region of this adapter protein (20). FADD recruitment is essential for downstream signaling of programmed cell death triggered through the Fas receptor (21,22). When overexpressed, Fas and FADD interact constitutively (23). As shown in Figure 6, cotransfection of the full-length Fas molecule Fas(1–319)-CFP with the FADD(DD)-YFP fusion protein, but not the control YFP fusion protein, showed significant FRET. Microscopic analysis of these cells showed significant but not complete recruitment of FADD-YFP to the plasma membrane (data not shown), indicating that FRET can still be detected even when only a subpopulation of molecules are colocalized.

DISCUSSION

In this report, receptor-specific association of TNFRs was demonstrated using flow cytometric analysis of FRET. We showed that this technique could monitor intracellular as well as extracellular molecular interactions. Thus, flow cytometric analysis of FRET using spectral variants of GFP provides a new and effective tool for screening close molecular associations in mammalian cells.

In designing the fusion proteins, several parameters appear to be critical for the success of the experiments. Efficient FRET requires both the fluorescence donor and acceptor to have sufficient quantum yield. The extinction coefficients, especially that of the acceptor, are also very important. In fact, the low quantum yield of the blue fluorescent protein (BFP) makes it a less than ideal FRET donor. It is also important to use the brightest CFP population as a control for setting compensation, as it is more accurate. For the TNFR receptors, fluorescence of fusions at the NH_2-terminal are sensitive to the linker length. For both p60 and p80, it appears that the longer the linker between the PLAD and YFP, the stronger the fluorescence is. In fact, preliminary data suggest that increasing the linker length further to 22 amino acid residues (YFP_{22}-p60) will give rise to a much brighter NH_2-terminal p60 fusion (data not shown). This may reflect a requirement of the CFP and YFP moieties for a certain distance to fold properly. It should be noted, however, that ECD fusions with longer linkers (CFP_{15}-p60 and YFP_{15}-p60) yielded no FRET, probably because of the increased distance between the CFP and YFP moieties (data not shown). In contrast to the ECD fusions, intracellular fusions of CFP

and YFP were found to be far less sensitive to the length of the linker (data not shown).

Another consideration in designing FRET fusion proteins is whether the fusion will alter the biological function of the protein. For p60 and p80 TNFRs, the NH_2-terminal fusion of CFP or YFP impairs ligand binding of the receptor. In fact, this is the reason why no ligand-dependent changes in FRET were observed between CFP_2-p60 and YFP_2-p60 (data not shown). On the other hand, the placement of CFP and YFP in the intracellular region of the receptor yielded ligand-dependent changes in FRET, and the Fas(1–317)-CFP fusion protein was still able to bind to the adapter protein FADD, as does the wild-type molecule. Although the different behavior of the intracellular and ECD receptor fusions can be attributed to suboptimal orientation of the CFP and YFP moieties, it nevertheless highlights the importance of achieving proper folding of the fusion proteins as well as avoiding steric hindrance with normal association functions.

Flow cytometric analysis of FRET complements the microscopic FRET analysis technique as it allows the collection of thousands of events in a short time, and can be easily adapted in many laboratories equipped with flow cytometers. Because of its ability to analyze large number of cells in a short time, it can be employed as a screening tool for drugs that inhibit important cellular interactions. Flow cytometric FRET analysis may also be a powerful way to screen large number of proteins for in vivo interactions, a task that is becoming increasingly necessary to understand the functions of the thousands of novel proteins identified through genomic approaches.

ACKNOWLEDGMENTS

We thank T. Waldmann and H. Metzger for discussions of FRET and receptor association, and D. Stephany for assistance on flow cytometry. F.K.C. was supported by a Miriam and Benedict Wolf/Cancer Research Institute fellowship.

LITERATURE CITED

1. Forster T. Energiewanderung und Fluoreszenz. Naturwissenschaften 1946;6:166–175.
2. Forster T. Zwischenmolekulare Energiewanderung und Fluoreszenz. Ann Phys (Leipzig) 1948;2:55–75.
3. Szollosi J, Matyus L, Tron L, Balazs M, Ember I, Fulwyler MJ, Damjanovich S. Flow cytometric measurements of fluorescence energy transfer using single laser excitation. Cytometry 1987;8:120–128.
4. Szollosi J, Tron L, Damjanovich S, Helliwell SH, Arndt-Jovin D, Jovin TM. Fluorescence energy transfer measurements on cell surfaces: a critical comparison of steady-state fluorimetric and flow cytometric methods. Cytometry 1984;5:210–216.
5. Tron L, Szollosi J, Damjanovich S, Helliwell SH, Arndt-Jovin DJ, Jovin TM. Flow cytometric measurement of fluorescence resonance energy transfer on cell surfaces. Quantitative evaluation of the transfer efficiency on a cell-by-cell basis. Biophys J 1984;45:939–946.
6. Tron L, Szollosi J, Damjanovich S. Proximity measurements of cell surface proteins by fluorescence energy transfer. Immunol Lett 1987; 16:1–9.
7. Mittler RS, Goldman SJ, Spitalny GL, Burakoff SJ. T-cell receptor-CD4 physical association in a murine T-cell hybridoma: induction by antigen receptor ligation. Proc Natl Acad Sci U S A 1989;86:8531–8535.
8. Rojo JM, Saizawa K, Janeway CA Jr. Physical association of CD4 and the T-cell receptor can be induced by anti-T-cell receptor antibodies. Proc Natl Acad Sci U S A 1989;86:3311–3315.
9. Carraway KLD, Cerione RA. Comparison of epidermal growth factor (EGF) receptor-receptor interactions in intact A431 cells and isolated plasma membranes. Large scale receptor micro-aggregation is not detected during EGF-stimulated early events. J Biol Chem 1991;266: 8899–8906.
10. Damjanovich S, Bene L, Matko J, Alileche A, Goldman CK, Sharrow S, Waldmann TA. Preassembly of interleukin 2 (IL-2) receptor subunits on resting Kit 225 K6 T cells and their modulation by IL-2, IL-7, and IL-15: a fluorescence resonance energy transfer study. Proc Natl Acad Sci U S A 1997;94:13134–13139.
11. Guo C, Dower SK, Holowka D, Baird B. Fluorescence resonance energy transfer reveals interleukin (IL)-1- dependent aggregation of IL-1 type I receptors that correlates with receptor activation. J Biol Chem 1995;270:27562–27568.
12. Tsien RY. The green fluorescent protein. Annu Rev Biochem 1998; 67:509–544.
13. Day RN. Visualization of Pit-1 transcription factor interactions in the living cell nucleus by fluorescence resonance energy transfer microscopy. Mol Endocrinol 1998;12:1410–1419.
14. Mahajan NP, Linder K, Berry G, Gordon GW, Heim R, Herman B. Bcl-2 and Bax interactions in mitochondria probed with green fluorescent protein and fluorescence resonance energy transfer. Nat Biotechnol 1998;16:547–552.
15. Miyawaki A, Llopis J, Heim R, McCaffery JM, Adams JA, Ikura M, Tsien RY. Fluorescent indicators for Ca2+ based on green fluorescent proteins and calmodulin. Nature 1997;388:882–887.
16. Chan FKM, Chun HJ, Zheng L, Siegel RM, Bui KL, Lenardo MJ. A domain in TNF receptors that mediates ligand-independent receptor assembly and signaling. Science 2000;288:2351–2354.
17. Siegel RM, Frederiksen JK, Zacharias DA, Chan FKM, Johnson M, Lynch D, Tsien RY, Lenardo MJ. Fas preassociation required for apoptosis signaling and dominant inhibition by pathogenic mutations. Science 2000;288:2354–2357.
18. Chan FKM. The pre-ligand binding assembly domain: a potential target of inhibition of tumour necrosis factor receptor function. Ann Rheum Dis 2000;59 Suppl 1:I50–I53.
19. Chan FKM, Siegel RM, Lenardo MJ. Signaling by the TNF receptor superfamily and T Cell homeostasis. Immunity 2000;13:419–422.
20. Kischkel FC, Hellbardt S, Behrmann I, Germer M, Pawlita M, Krammer PH, Peter ME. Cytotoxicity-dependent APO-1 (Fas/CD95)-associated proteins form a death-inducing signaling complex (DISC) with the receptor. Embo J 1995;14:5579–5588.
21. Yeh WC, Pompa JL, McCurrach ME, Shu HB, Elia AJ, Shahinian A, Ng M, Wakeham A, Khoo W, Mitchell K, El-Deiry WS, Lowe SW, Goeddel DV, Mak TW. FADD: essential for embryo development and signaling from some, but not all, inducers of apoptosis. Science 1998;279: 1954–1958.
22. Zhang J, Cado D, Chen A, Kabra NH, Winoto A. Fas-mediated apoptosis and activation-induced T-cell proliferation are defective in mice lacking FADD/Mort1. Nature 1998;392:296–300.
23. Chinnaiyan AM, O'Rourke K, Tewari M, Dixit VM. FADD, a novel death domain-containing protein, interacts with the death domain of Fas and initiates apoptosis. Cell 1995;81:505–512.